Journal of Organometallic Chemistry 696 (2011) 2711–2719

Contents lists available at ScienceDirect

Journal of Organometallic Chemistry

journal homepage: www.elsevier.com/locate/jorganchem

Cyclometalated Ir(III) complexes containing *N*-aryl picolinamide ancillary ligands

Vadapalli Chandrasekhar [a,*], Bani Mahanti [a], Priyanka Bandipalli [b], Kotamarthi Bhanuprakash [b], Nisanth N. Nair [a]

[a] Department of Chemistry, Indian Institute of Technology Kanpur, Kanpur 208 016, India
[b] Inorganic and Physical Chemistry Division, Indian Institute of Chemical Technology, Hyderabad 500 607, India

ARTICLE INFO

Article history:
Received 19 February 2011
Received in revised form
6 April 2011
Accepted 11 April 2011

Keywords:
Cyclometalated
N-Aryl picolinamide
Absorption
Emission
Lifetime
Time dependent DFT

ABSTRACT

The reaction of the cyclometalated chloro-bridged iridium(III) dimer, $[(ppy)_2\ Ir(\mu\text{-}Cl)]_2$ (ppy − 2-phenyl pyridine) with *N*-aryl picolinamides (LH, LH−NO_2, LH−CH_3, LH−I, LH−F) resulted in the formation of neutral heteroleptic complexes $[Ir(ppy)_2L]$ (**1**), $[Ir(ppy)_2L\text{–}NO_2]$(**2**), $[Ir(ppy)_2L\text{–}CH_3]$(**3**), $[Ir(ppy)_2L\text{–}Cl]$(**4**) and $[Ir(ppy)_2L\text{–}F]$ (**5**). These complexes contain a six-coordinate iridium with a 2C, 4N coordination environment. The *N*-aryl picolinamide ligands are deprotonated during complexation and the resulting amidates bind to iridium in a chelating manner (*N*, *N*). Optical spectroscopic studies revealed that the complexes **1**–**5** exhibited intense $\pi\rightarrow\pi^*$ absorptions in the ultraviolet region. In addition low energy transitions due to ^{1}MLCT, ^{1}LLCT and ^{3}MLCT are also seen. The emission spectra of **1**–**5**, upon excitation at 450 nm, show a single emission with a λ_{max} around 513 nm. The lifetimes of this emission are in between 7.4 and 9.6 μs while the quantum yields are quite high and range from 0.2 to 0.5. Based on density functional theory (DFT) calculations on **1** and **3,** the three highest occupied orbitals are composed of ligand π orbitals mixed with Ir-d orbitals while the three lowest unoccupied orbitals are mostly π orbitals of the ligands. From the time dependent DFT calculations it is revealed that the lowest energy electronic singlet and triplet excitations are a mixture of MLCT and LLCT.

1. Introduction

In recent years there has been considerable research activity that has been directed towards organometallic cyclometalated Ir(III) complexes [1]. This interest stems from both practical and academic viewpoints. Due to a strong spin-orbit coupling cyclometalated Ir(III) complexes exhibit phosphorescence with moderate to high quantum yields and because of this such complexes have been viewed as potential phosphorescent dopants in organic light-emitting diode (OLED) devices [2]. Other applications of these complexes are varied and include light-emitting electrochemical cells [3], electrogenerated chemiluminescence [4], photoinduced hydrogen production [5], photoelectrochemical solar cells [6] as well as phosphorescent probes/markers in biological systems [7]. From an academic point of view there has been considerable interest in unraveling and understanding the precise mechanism of emission of these complexes including the details of the various excited state energy levels that are involved in this process. Theoretical studies, particularly those based on density functional theory (DFT) have been particularly useful in conjunction with experiments to make steady progress in the understanding of the photophysical processes in cyclometalated Ir(III) complexes [8].

In spite of significant progress, considerable amount of work still remains to be done before one can settle down on the ideal families of cyclometalated Ir(III) complexes that can be used in various practical devices. One of the ways of modulating the properties of the complexes vis-à-vis their molecular structures is by the choice of an appropriate cyclometalating (*C^N*) ligand and an ancillary ligand leading to both homoleptic $[Ir(C^N)_3]$ [9] or heteroleptic $[Ir(C^N)_2L]^{n+}$ ($n = 0, 1$) complexes [10]. While the cyclometalating ligand of choice mostly has been a 2-phenyl pyridine (ppy) based ligand, ancillary ligands have been varied from acetylacetonate to tetrazole. However, in spite of this attention to the ancillary ligand, surprisingly there have been very few attempts to utilize amide ligands [11]. One of these reports the generation of the amide linkage on the cyclometalated Ir(III) complex, in situ, by a photochemical singlet oxygen-induced process [11a]. On the other hand amide ligands have been extensively used in transition metal chemistry [12] and are known to stabilize higher oxidation states as well as impart stability to the complexes. For example, recently, amide ligand complexes of Pd(II) have been reported. These complexes were shown to be especially stable in solution and serve as excellent catalysts in C–C bond formation reactions [13]. In view of this we have explored the possibility of incorporating amide ligands (LH,

* Corresponding author. Tel.: +91 512 259 7259; fax: +91 521 259 0007x7436.
E-mail address: vc@iitk.ac.in (V. Chandrasekhar).

0022-328X/$ – see front matter © 2011 Elsevier B.V. All rights reserved.
doi:10.1016/j.jorganchem.2011.04.011

LH–NO_2, LH–CH_3, LH–Cl, LH–F) to form neutral heteroleptic complexes [Ir(ppy)$_2$L] (**1**), [Ir(ppy)$_2$L–NO_2](**2**), [Ir(ppy)$_2$L–CH_3](**3**), [Ir(ppy)$_2$L–Cl](**4**) and [Ir(ppy)$_2$L–] (**5**) where L and substituted-L are chelating (*N*, *N*) amidate ligands while the cyclometalating ligand is the phenyl pyridine ligand (Scheme 1). Synthesis, structural studies, photophysical studies, theory and electrochemistry of these complexes are reported herein.

2. Results and discussion

2.1. Synthesis

The heteroleptic Ir(III) complexes **1**–**5** containing two cyclometalating 2-phenyl pyridine ligands and one deprotonated *N*-aryl picolinamide ligand were prepared by a sequential two step synthetic procedure (Scheme 1). The cyclometalated chloro-bridged iridium(III) dimer, [(ppy)$_2$ Ir(μ-Cl)]$_2$ was prepared by using the Nonoyama protocol; subsequent reaction of this iridium(III) dimer with sodium methoxide followed by reaction with *N*-aryl picolinamides afforded the neutral, monomeric, heteroleptic complexes **1**–**5** in good yields (see Experimental Section). The *N*-aryl picolinamide ligands undergo deprotonation and the resultant monomeric ligands bind to the Ir(III) center by a *N*, *N* chelating mode (see below for molecular structures). Infrared spectroscopic studies support the deprotonation at the ligands as revealed by the disappearance of the υ_{N-H} in the complexes (in the ligands the υ_{N-H} is seen between 3300 cm^{-1} and 3340 cm^{-1}). The amide C=O stretch, observed between 1670 and 1687 cm^{-1} in the uncoordinated ligands, is also found to be shifted to around 1600 cm^{-1} in all the complexes indicating the influence of coordination on the ligand. ESI-MS spectra of all the five complexes reveals the presence of the molecular ion peak $[M+H]^+$; in addition in all the cases peaks due to $[2M+H]^+$ are also seen.

Thermogravimetric analyses were performed on all the complexes to ascertain their thermal stability. It is known that simple Ir(III) complexes such as Ir(acac)$_3$ suffer thermal degradation at fairly low temperatures (~243 °C) [8a]. In the present instance all the compounds remain intact up to approximately 300 °C. Varied amounts of degradation are found after this stage, ranging from 5% at 323 °C for complex **5** to 20% at 335 °C for **1** (see Supporting Information). At 700 °C the char yields of compounds **1**–**5** are respectively 21.0%, 61.4%, 50.6%, 42.0 and 60.0% indicating high thermal stability of these complexes. A representative TGA curve is shown in Fig. 1 (see Supporting Information for the TGA curves of other complexes).

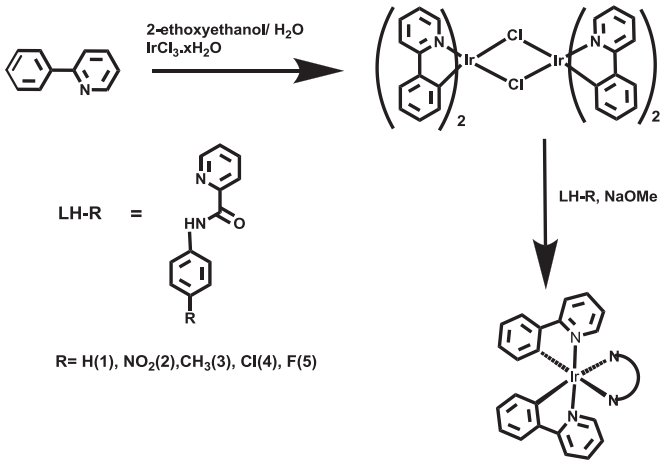

Scheme 1. Synthesis of iridium complexes.

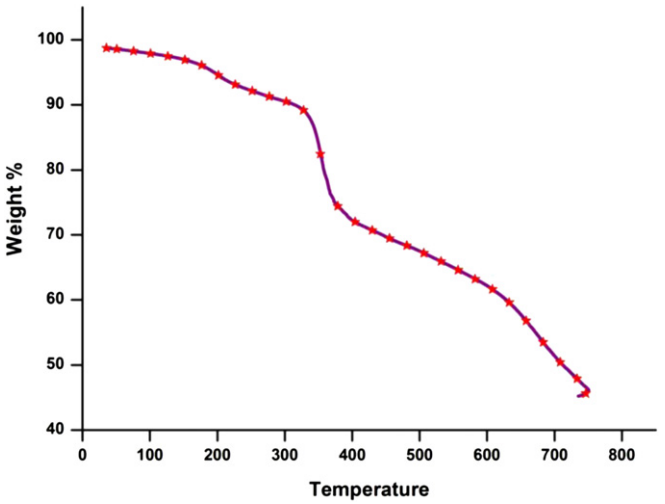

Fig. 1. Thermogravimetric curve of **3**.

2.2. Molecular structures of *1*, *3*, *4* and *5*

The molecular structures of these heteroleptic complexes as ascertained by ESI-MS and analytical data (see Experimental Section) were confirmed by an X-ray crystallographic study of **1**, **3**, **4** and **5**. While the molecular structure of **2** could be ascertained from its crystallographic study the poor quality of the X-ray data precludes any discussion on its bond parameters.

Single crystals of **1, 3, 4** and **5** were obtained from their dichloromethane solutions by layering them with a few drops of methanol. Compounds **1**, **3** and **4** crystallize in monoclinic space groups while compound **5** crystallizes in a triclinic space group. The asymmetric unit of compound **5** contains two independent molecules. The crystallographic data for these compounds are summarized in Table 1.

ORTEP diagrams of **1, 3, 4** and **5** are given in Fig. 2. Selected bond parameter data for compounds **1** and **3** are summarized in Tables 2 and 3 while for compounds **4** and **5** is given in supporting information (Tables S1 and S2). All the four compounds are mononuclear, neutral, cyclometalated Ir(III) complexes. The metal center in each complex is bound to three chelating ligands, two phenyl pyridine ligands (C^N) and one picolinamide ligand (N^N). Thus, the iridium center in each complex has a 2C, 4N coordination environment. The coordination geometry around the iridium center is distorted octahedral with the nitrogen atoms of the phenyl pyridine ligands occupying *trans* positions while the two carbon atoms of these ligands preferring the *cis* orientation. This ligand geometry is similar to that found in the precursor [(ppy)$_2$Ir(μ-Cl)]$_2$ suggesting that the formation of the amide complexes involves a simple replacement of the bridging chlorine atoms without causing disturbance to the coordination of the cyclometalating 2-phenyl pyridine unit. A similar behavior is observed in other cyclometalated Ir(III) complexes containing ancillary ligands.

In general picolinamides are known to bind to transition metal ions in two forms (a) an amide form, where the ligand is neutral and is a *N*, *O* donor and (b) an amidate form where the ligand is deprotonated and functions as a *N*, *N* donor (Chart 1). In the current instance in all the complexes the coordination mode of the picolinamide corresponds to the amidate form. As described above, this mode of coordination has also been confirmed by infrared spectroscopy. Interestingly prior to this work, in the literature, only three precedents of amide coordination to cyclometalated Ir(III) complexes are known. In all cases amidate form of coordination has been observed [11].

An inspection of the bond parameters reveals that the Ir–N distances involving the chelating amide ligand (*N^N*) are slightly

Table 1
X-ray crystallographic data for compounds **1**, **3**, **4** and **5**.

Parameters	1	3	4	5
Empirical formula	$C_{35}H_{29}IrN_4O_2$	$C_{35}H_{27}IrN_4O$	$C_{34}H_{24}ClIrN_4O$	$C_{72}H_{64}F_2Ir_2N_8O_6$
Formula weight	729.82	711.81	732.22	1559.71
Temperature (K)	153(2)	100(2)	100(2)	100(2)
Wavelength (Mo k_α)	0.71073 Å	0.71073 Å	0.71073 Å	0.71073 Å
Crystal system	Monoclinic	Monoclinic	Monoclinic	Triclinic
Space group	$P2_1/c$	$P2_1/n$	$P2_1/n$	$P1$
a/Å	8.6865(10	16.265(4)	16.247(4)	13.536(4)
b/Å	11.5764(13)	10.204(3)	10.150(3)	13.611(4)
c/Å	27.756(3)	17.973(5)	18.080(4)	17.926(5)
α(deg)	90	90	90	91.721(4)
β(deg)	92.136(2)	113.273(4)	113.696(4)	108.355(4)
γ(deg)	90	90	90	91.392(4)
Volume/Å^3	2789.2(5)	2740.2(12)	2730.3(12)	3131.1(14)
Z	4	4	4	2
Calculated density (g/cc)	1.738	1.725	1.781	1.654
Absorption coefficient (mm^{-1})	4.828	4.909	5.024	4.313
F (000)	1440	1400	1432	1544
θ range for data collection (deg)	2.29–26.00	2.17–26.00	2.18–26.00	2.14–25.00
Reflections collected	15236	14894	14748	16207
Independent reflections	5454 [R(int) = 0.0374]	5347 [R(int) = 0.0495]	5320 [R(int) = 0.0555]	10860 [R(int) = 0.0323]
Parameters	381	371	370	817
Goodness-of-fit on F^2	1.046	1.050	1.016	1.048
Final R indices	0.0321	0.0366	0.0383	0.0497
R indices (all data)	0.0414	0.0482	0.0472	0.0712
Largest diff. peak and hole	2.262 and −0.655 (e. Å^{-3})	3.213 and −1.123 (e. Å^{-3})	3.131 and −1.526 (e. Å^{-3})	2.660 and −1.487 (e. Å^{-3})

longer [2.112(7)-2.179(7) Å] than those involving the chelating 2-phenyl pyridine (*C^N*) ligand [2.031(6)-2.050(7) Å]; the strong *trans* influence of the metalated carbon atom of the 2-phenyl pyridine group presumably is responsible for the longer Ir–N distances involving the amide ligand. In each of the complexes the C–O distance is significantly shorter than the C–N distance, except in one of the molecules present in complex **5** where the difference between these two bond types is not very large [C–O, 1.280(10); C–N, 1.320(11)]. Among the bond angles involving the *trans* substituents the N–Ir–N bond angles are the most linear while the C–Ir–N bond angles deviate more from the ideal values. Overall the bond parameters found in the present instance are comparable with other cyclometalated Ir(III) complexes containing a similar ligand environment [14].

2.3. Photophysical properties

The utility of cyclometalated Ir(III) complexes as phosphorescent dopants in OLED devices is mainly due to the strong spin-orbit coupling exhibited by the heavy metal center which facilitates access to the triplet excited states by an efficient mixing of singlet and triplet excited states. As seen previously in complexes of the type $[(ppy)_2Ir(acac)]$ [15], in the present instance also, intense absorption due to the 2-phenyl pyridine ligands ($\pi \rightarrow \pi^*$) is seen. The $\pi \rightarrow \pi^*$ absorptions due to the ancillary ligands overlap with those of the 2-phenyl pyridine ligands(see Supporting Information for absorption spectra of ancillary ligands). These absorption bands are in the ultraviolet region with high extinction coefficients (Fig. 3, Table 4). The low energy bands which are due to ^{1}MLCT, ^{1}LLCT, ^{3}MLCT (see also the results from DFT calculations in the following section) resemble those that have been observed previously for $[(ppy)_2Ir(acac)]$, $[Ir(ppy)_2(L–N, N)]$ (PF_6), $[Ir(ppy)_2$ $(\eta^2$-XZY)] [15,16]. Interestingly, the variation of the ancillary ligand in complexes **1**–**5** does not lead much variation in the λ_{max} values although the extinction coefficient does change (Fig. 3). The emission spectra of **1**–**5** (excitation wavelength, 450 nm) shows a single emission with a λ_{max} around 513 nm (see Fig. 4 for a representative emission spectrum). The lifetimes of this emission fall in the microsecond region (7.4–9.6 μs) suggesting the phosphorescent nature of this emission. These lifetimes may be compared to those observed in literature [15]. The quantum yields calculated with reference to quinine sulfate, are quite high and range from 0.2 to 0.5 (Table 4). The shape of the emission spectra in terms of the lack of vibronic fine structure indicates that the emission occurs from a charge-transfer excited state [17]. This hypothesis is corroborated by density functional theory based calculations (see below).

2.4. DFT and TDDFT studies

To understand the ground and excited state properties we have performed DFT and TDDFT calculations for compounds **1** and **3**. The results for **1** are discussed below while that of **3** are given in the Supporting Information.

The main optimized geometry parameters of **1** in the ground state together with X-ray crystal diffraction data are given in Table S3 of supporting information which shows that the optimized bond parameters are well consistent with the corresponding experimental values in case of PBE0 function.

To gain insight into the electronic structure of complex **1** we report in Table 5 the important molecular orbital composition and in Fig. 5 the isodensity surface plots of some selected molecular orbitals. The calculations show that HOMO is centered on Ir atom and the ancillary ligand whereas LUMO is a π^* orbital centered mainly on the cyclometalating ligand (phenyl pyridine). H − 1 is centered on Ir atom and cyclometalating ligand whereas L + 1 is centered mainly on the ancillary ligand. H − 2 is composed of Ir atom together with contributions from both cyclometallating as well as ancillary ligand, however L + 2 is composed of cyclometallating ligand only. In short 17–43% of the three highest HOMO's are Ir-d orbitals whereas LUMO and next two unoccupied orbitals are mostly π^* orbitals of ligands with negligibly small involvement of Ir orbitals.

TDDFT calculations were employed to understand the nature of the excited states and examine the vertical excitation energies. TDDFT calculation in the framework of the PCM model for dichloromethane solvent gives a better agreement with experimental one. After testing different DFT functional we found B3LYP/LANL2DZ/6-31G* gave satisfactory description of UV–Vis

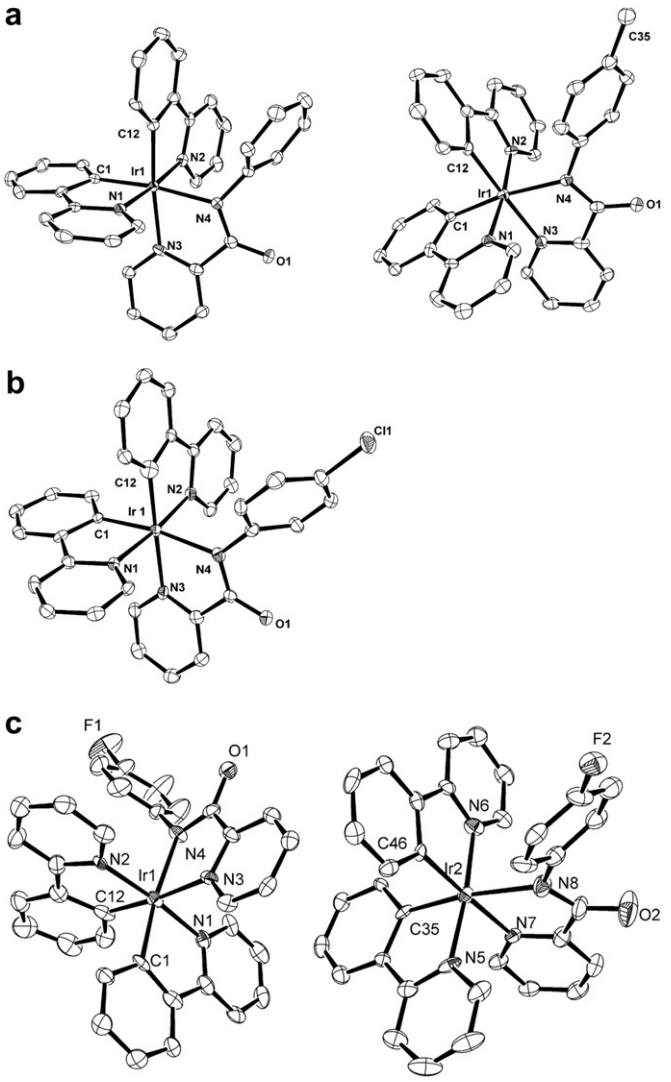

Fig. 2. (a) ORTEP diagrams of **1** and **3** with thermal ellipsoids at 50% probability limit. H atoms and solvent molecules are omitted for clarity, (b): ORTEP diagram of **4** with thermal ellipsoids at 50% probability limit. H atoms are omitted for clarity, (c): ORTEP diagram of **5** with thermal ellipsoids at 50% probability limit. H atoms and solvent molecules are omitted for clarity. (One asymmetric unit contains two molecules in **5**).

absorption determined experimentally (Tables 6 and 7 shows first 10 singlet and 5 triplet transitions using PBE0 and B3LYP functional). For the two methods tested we were successful in reproducing the main spectral features and their relative intensities with minor deviations from one another. (Fig. S8 of supporting information shows simulated UV–Vis spectra at the B3LYP/LANL2DZ/6-31G* level).

Table 2
Selected bond parameters of **1**.

Ir(1)–N(1)	2.048(4)	Ir(1)–N(2)	2.046(4)
Ir(1)–N(3)	2.141(4)	Ir(1)–N(4)	2.147(4)
Ir(1)–C(1)	2.016(5)	Ir(1)–C(12)	2.006(5)
N(4)–C(28)	1.328(6)	C(28)–O(1)	1.261(5)
N(3)–Ir(1)–N(4)	75.58(14)	C(12)–Ir(1)–N(2)	80.13(17)
C(1)–Ir(1)–N(1)	81.03(17)	N(2)–Ir(1)–N(3)	97.87(15)
C(12)–Ir(1)–N(1)	95.09(17)	C(12)–Ir(1)–N(4)	98.64(16)
N(2)–Ir(1)–N(1)	175.00(15)	C(12)–Ir(1)–N(3)	174.08(16)
C(1)–Ir(1)–N(4)	172.60(16)		

Table 3
Selected bond parameters of **3**.

Ir(1)–N(1)	2.038(4)	Ir(1)–N(2)	2.032(4)
Ir(1)–N(3)	2.148(4)	Ir(1)–N(4)	2.153(4)
Ir(1)–C(1)	2.005(5)	Ir(1)–C(12)	2.001(5)
N(4)–C(28)	1.347(7)	C(28)–O(1)	1.247(6)
N(3)–Ir(1)–N(4)	76.53(17)	C(12)–Ir(1)-N(2)	80.5(2)
C(1)–Ir(1)–N(1)	80.6(2)	N(2)–Ir(1)–N(3)	99.56(16)
C(12)–Ir(1)–N(1)	95.0(2)	C(12)–Ir(1)–N(4)	101.48(19)
N(2)–Ir(1)–N(1)	174.31(17)	C(12)–Ir(1)–N(3)	178.01(18)
C(1)–r(1)–N(4)	171.00(18)		

From the transition character it is found that the three lowest energy singlet excitations are predominantly from the HOMO level. HOMO is composed of d orbitals of Ir and ancillary ligand orbitals. This suggests that the lowest energy transitions are a mixture of MLCT and LLCT. To account for the weak band experimentally found at 481 nm we looked at the singlet–triplet excitations (given in Table 7), the calculated one is obtained at 483 nm for PBE0 and 497 nm for B3LYP. According to these results T1 states can also be assigned as a mixture of MLCT and LLCT type transitions. Thus DFT provides evidence that luminescence observed in complex **1** originates from Ir perturbed ligand-centered transitions.

To theoretically confirm that the substitutions on the phenyl ring of the N-aryl picolinamide ligand have little effect on the emission spectra, we have also looked at the molecular orbitals and electronic excitations of **3**, where a methyl substitution is present. For **3**, the calculated excitation energies of singlet and triplet, and the participating orbitals are quantitatively and qualitatively the same as that of **1** (see Supporting Information), which is in accordance with the experimental observation. Overall our computational investigation basically confirms the similarity of the optical properties of all the complexes **1**–**5**.

2.5. Electrochemical studies

Cyclic voltammetric studies were performed to study the electrochemical properties of these complexes in dry CH_2Cl_2 using 1 mM concentration of the complexes and 0.1 M tetrabutylammonium hexaflorophosphate as the supporting electrolyte. These results are summarized in Table 8. All the redox events have been found to be quasi-reversible. Representative cyclic voltammograms for complexes **2** and **5** are shown in Fig. 6.

Two consecutive oxidation processes are observed for **1, 3, 4** and **5**, however, only a single oxidation peak was observed for **2** in this range. The first oxidation peak is attributed to the metal center with a substantial contribution from the ligands. DFT calculations (see above) also indicate that HOMO's consist of a mixture of metal (d) and ligand (π) orbitals. The second oxidation observed for compounds **1**, **3**, **4**, **5** is not metal-centered, as further oxidation to

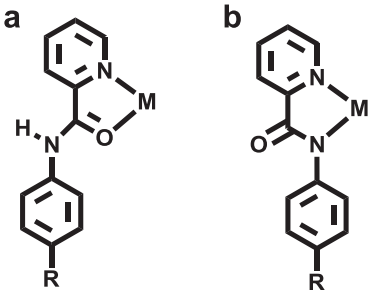

Chat 1. Coordination modes of *N*-aryl picolinamide ligands: (a) amide form; *N*, *O* donor (b) amidate form, *N*, *N* donor.

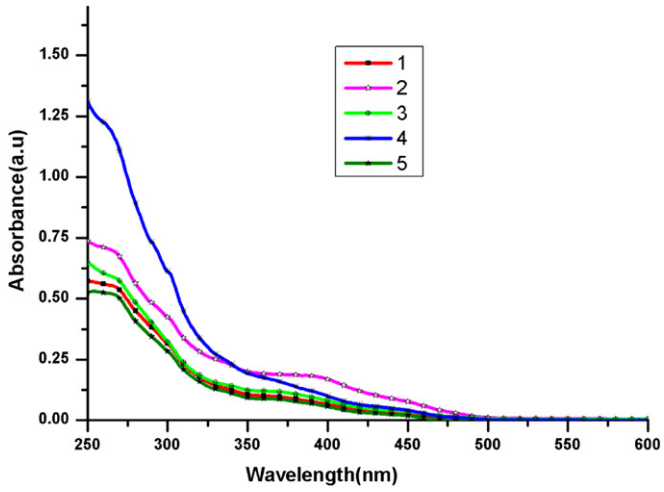

Fig. 3. Absorption spectra of **1**–**5**.

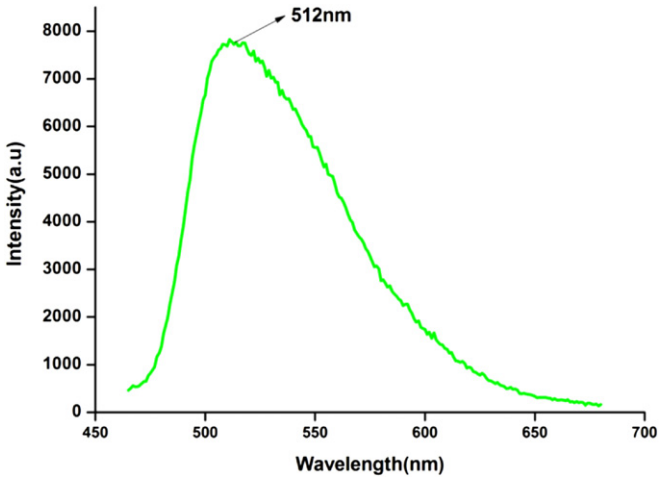

Fig. 4. Emission spectrum of **3**.

an Ir(IV) species is unlikely. Based on cyclic voltammetric studies of mer-Ir(ppy)$_3$ [18a] where oxidation of the 2-phenyl pyridine ligand does not occur below 1.65 V (vs Ag/AgCl), in the current instance the second oxidation is attributed to be on the *N*-aryl picolinamide ligand. This assignment also has literature support [18]. A reduction event was observed only for complex **2** which occurs on the coordinated amide ligand, more specifically due to the formation of nitro-radical complex [19].

3. Conclusions

In conclusion, we have prepared and characterized neutral cyclometalated Ir(III) complexes containing *N*-aryl picolinamide ligand, [Ir(ppy)$_2$L] (**1**), [Ir(ppy)$_2$L–NO$_2$] (**2**) [Ir(ppy)$_2$L–CH$_3$] (**3**) [Ir(ppy)$_2$L–Cl] (**4**) and [Ir(ppy)$_2$L–F] (**5**) where L and substituted-L are chelating (*N*, *N*) amidate ligands while the cyclometalating ligand is the 2-phenyl pyridine ligand. The use of amide ligands in cyclometalated Ir(III) complexes is sparse and the current study reveals the effectiveness of these ligands in the preparation of heteroleptic organometallic Ir(III) complexes. Complexes **1**–**5** revealed absorptions as a result of MLCT and LLCT. Further, all of these complexes emit in the green at ~513 nm with moderate to high quantum yields. DFT and TDDFT studies were carried out on **1** and **3** to throw light on the nature of the frontier orbitals involved in the absorption and emission process. The three HOMO's contain contributions from both ligand and iridium d orbitals while the three LUMO's are predominantly ligand based. Calculations also confirmed the nearly identical optical properties for various substitutions in N-aryl picolinamide ligand. Lifetime measurements indicate that the emissions are in the range of 7.4–9.6 μs supporting the phosphorescent nature of the emission. Electrochemical studies indicate two quasi-reversible oxidation events; the first of these occurs on a mixture of iridium-ligand orbitals. The second oxidation is ancillary ligand-centered. For **2**, however, only a single oxidation is seen, presumably because the nitro substituent on the amide ligand makes the ligand more resistant to oxidation. On, the other hand **2** undergoes a nitro-group centered reduction process.

4. Experimental section

4.1. General

All procedures involving Ir(III) complexes were carried out under a nitrogen gas atmosphere using Schlenk techniques. 2-Phenyl pyridine was purchased from Aldrich Chemical Company, USA and was used as such without further purification. Iridium chloride was purchased from Arora Matthey, Kolkata, India. Other chemicals were purchased from S. D. Fine-Chemicals, Mumbai, India. Solvents were purified by conventional methods and were freshly distilled under nitrogen atmosphere prior to use according to standard procedures [20]. Sodium methoxide was freshly prepared and used in the reactions. Reactions were monitored by TLC with Merck precoated plates.

4.2. Instrumentation

ESI-MS analyses were performed on a Waters Micromass Quattro Micro triple quadrupole mass spectrometer. Electrospray ionization (positive ion, full scan mode) was done using acetonitrile or methanol as the solvent while nitrogen gas used for desolvation. Capillary voltage was maintained at 2.5–2.7 kV and cone voltage was kept at approx 30 kV. Thermogravimetric analysis was carried out on a Perkin Elmer Pyris 6 Thermogravimetric analyzer at

Table 4
Photophysical properties of **1**–**5** at 25 °C.

Complex	Absorption[a] λ_{max} (nm); 10^{-4} ϵ (M^{-1} cm^{-1})	Emission[a] λ_{max} (nm)	τ (μs)	Φ[b]
1	266(5.5), 337(sh, 1.2), 368(sh, 0.9), 446(sh, 0.31), 481(sh, 0.08)	514	9.59	0.51
2	265(6.9), 334(sh, 2.4), 392(sh, 1.8), 446(sh, 0.79), 479(sh, 0.28)	513	7.36	0.53
3	267(5.8), 339(sh, 1.43), 375(sh, 1.11), 448(sh, 0.39), 480(sh, 0.15)	512	9.9	0.26
4	259(12.2), 336(sh, 2.49), 363(sh, 1.69), 447(sh, 0.43), 480(sh, 0.13)	512	9.96	0.49
5	252(5.3), 338(sh, 1.1), 366(sh, 0.8), 444(sh, 0.2)	514	9.01	0.23

[a] Absorption and emission spectral data of all the complexes were recorded in dichloromethane solution at room temperature (absorption in 10^{-5} M solution; emission in 10^{-4} M solution, λ_{exc} = 450 nm); "sh" denotes a shoulder.
[b] Quantum yields are measured with respect to quinine sulfate in 1.0 N sulfuric acid solution whose emission yield was Φ = 0.54 ± 0.2 (λ_{exc} = 350 nm).

Table 5
Molecular Orbital composition (%) in the ground state at the PBE0/LANL2DZ/6-31G* level for 1.

Orbital	Energy (eV)	Ir	Ir(d)	Cyclometallating ligand (L_C)	Ancillary ligand (L_A)	Main bond nature
LUMO + 3	−0.960	3.5	0.3	66.3	30.2	L_C (54.6%) + L_A (30.2%)
LUMO + 2	−1.181	5.9	4.2	90.7	3.4	L_C (90.7%)
LUMO + 1	−1.315	4.8	3.1	7.8	87.4	L_A (87.4%)
LUMO	−1.420	4.2	2.4	88.7	7.1	L_C (88.7%)
HOMO	−5.018	17.5	16.6	7.7	74.8	Ir-d (16.6%) + L_A (74.8%)
HOMO − 1	−5.430	43.6	42.7	47.7	8.8	Ir-d (42.7%) + L_C (47.7%)
HOMO − 2	−6.005	20.3	19.1	23.8	55.9	Ir-d (19.1%) + L_C (23.8%) + L_A (55.9%)
HOMO − 3	−6.106	5.5	4.8	73.2	21.3	L_C (73.2%) + L_A (21.3%)

a heating rate of 10 °C/min under argon. Melting points were recorded using a JSGW melting point apparatus. None of the complexes melted up to 200 °C. ^{1}H NMR spectra were obtained on a JEOL-DELTA 2500 model spectrometer using $CDCl_3$ as the solvent and TMS as the reference. NMR data are reported in ppm. Elemental analyses were carried out using a Thermoquest CE instruments CHNS-O, EA/110 model. The analyses of compounds were carried out on fully dried samples. IR spectra were recorded as KBr pellets from 4000 to 400 cm^{-1} on a Bruker FT-IR Vector 22 model. UV–visible spectra were recorded on a Perkin Elmer-Lambda 20 UV–visible spectrometer in 1×10^{-5} M dichloromethane solution. The steady state emission spectra were measured using a Fluorolog FL3-21 (Horiba Jobin Yvon) spectrofluorimeter using 1×10^{-4} M dichloromethane solution. The excited state lifetimes were measured with the same system under microsecond Xenon flash lamp operating conditions. The best fit was assessed based on the parameter χ^2, which was close to 1.0 for all the samples. Quantum yields were measured with reference to quinine sulfate in 1.0 N sulfuric acid solution with an emission yield of $\Phi = 0.54 \pm 0.2$ (λ_{exc} = 350 nm) [21]. The quantum yields were then calculated using the following expression:

$$\Phi_U = \Phi_R(A_U/A_R)(n_{U^2}/n_{R^2})$$

In the above equation, the subscripts *U* and *R* denote sample and reference respectively, Φ is the fluorescence quantum yield, A is the integrated area under the corrected fluorescence spectra, n is the refractive index of the solvent.

Cyclic voltammetric studies were performed on a BAS Epsilon electrochemical workstation using a platinum working electrode, an Ag/AgCl reference electrode (3 M NaCl), and a platinum-wire counter electrode. All measurements were performed in 0.1 M [*n*-Bu_4N][PF_6] in dry dichloromethane using 1 mM concentrations of the complexes. The ferrocene/ferrocenium couple was taken as internal standard; $E_{1/2}$ = +0.51(70) V versus Ag/AgCl under the same experimental conditions.

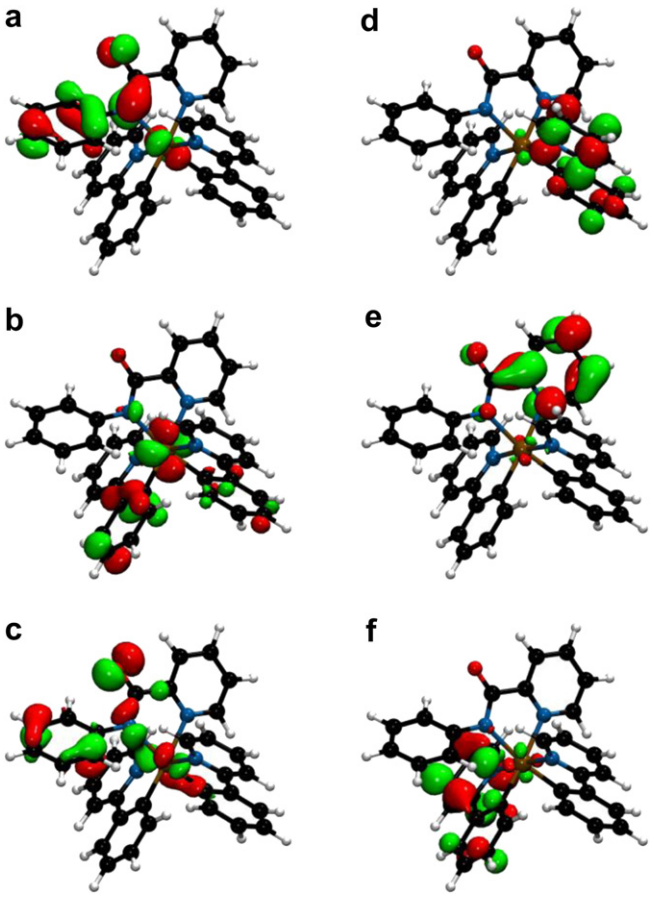

Fig. 5. Relevant molecular orbitals of **1** obtained from DFT calculations drawn at an isovalue of ±0.05 (red/green surfaces): (a) HOMO (b) HOMO-1 (c) HOMO-2 (d) LUMO (e) LUMO+1 (f) LUMO+2. Color codes of atoms: blue (N), black (C), white (H), red (O), brown (Ir). "(For interpretation of the references to colour in this figure legend, the reader is referred to the web version of this article.)"

4.3. X-ray structural analysis

Important crystallographic data for compounds **1**, **3**, **4** and **5** are given in Table 1. Single crystals of **1**, **3**, **4** and **5** suitable for X-ray crystallography were obtained by slow evaporation of their dichloromethane solutions that have been layered with a few drops of methanol. X-ray data were collected on a CCD Bruker SMART APEX diffractometer at 100(2) K using a graphite monochromated Mo K_α radiation (K_α = 0.71073 Å). No decomposition of the crystal occurred during data collection. The program SMART [22] was used for collecting frames of data, indexing reflection, and determining lattice parameters, SAINT for integration of the intensity of

Table 6
Singlet excited states of **1** using PBE0/LANL2DZ/6-31G* and B3LYP/LANL2DZ/6-31G* using PCM solvation model.

States	PBE0/LANL2DZ/6-31G*		B3LYP/LANL2DZ/6-31G*	
	λ (nm)	f	λ (nm)	f
S1	401.35	0.0226	424.16	0.0244
S2	400.12	0.0324	422.86	0.0151
S3	386.58	0.0013	407.39	0.0013
S4	372.81	0.0288	393.22	0.0362
S5	370.98	0.0448	391.54	0.0294
S6	354.36	0.0345	372.38	0.0284
S7	342.28	0.0241	363.60	0.0251
S8	324.48	0.0100	343.20	0.0081
S9	321.82	0.0073	341.06	0.0065
S10	318.84	0.0081	336.04	0.0134

Table 7
Triplet excited states of **1** using PBE0/LANL2DZ/6-31G* and B3LYP/LANL2DZ/6-31G* using PCM solvation model.

States	PBE0/LANL2DZ/6-31G* λ (nm)	B3LYP/LANL2DZ/6-31G* λ (nm)
T1	483.80	497.41
T2	457.02	458.96
T3	451.70	450.36
T4	398.85	413.30
T5	391.72	403.84

reflections and scaling, SADABS [23] for absorption correction, and SHELXTL [24] for space group and structure determination and least-squares refinements on F^2. All non-hydrogen atoms were refined with anisotropic displacement parameters. Hydrogen atoms were fixed in geometrically calculated positions using a riding model and were refined isotropically. For complex **5**, one of the methanol molecules was found to be disordered. The carbon atom (C71) of the methanol molecule was disordered over two positions (C71A and C71B) with occupancies 0.70 and 0.30. The oxygen atom (O5) of the same methanol molecule was disordered over two positions (O5A and O5B) with occupancies 0.55 and 0.45.

4.4. Computational details

The ground state geometry of **1** was optimized by two different density functional theory (DFT) methods: Becke's LYP(B3LYP) exchange correlation functional [25] and gradient corrected correlation functional PBE0 [26]. PBE0 provides the best match with the geometrical X-ray data. Full geometry optimization without symmetry constraints were carried out in the gas phase for the singlet ground state (S_0) of **1**. The optimized geometry was confirmed to be potential energy minima by vibrational frequency calculation at the same level of theory as no imaginary frequencies were found. In the calculation, the quasi-relativistic pseudo-potentials of Ir atoms proposed by Hay and Wadt [27] with 17 valence electrons were used, and a double zeta quality basis set LANL2DZ was adopted. 6-31G* basis set was used on all the nonmetal atoms.

At the optimized geometry TDDFT calculations were performed by two different methods: PBE0/LANL2DZ/6-31G*, B3LYP/LANL2DZ/6-31G* in dichloromethane solution by means of PCM solvation model [28] as implemented in the Gaussian 03 program package. 60 singlet–singlet excitations and the lowest 10 single-t–triplet excitations at the S_0 optimized geometry allowed us to simulate a large (up to 250 nm) portion of the absorption spectrum and gain insight into the nature of the transitions giving rise to the low energy spectral region. The oscillator strengths of single-t–triplet transitions are set to zero due to neglect of spin-orbit coupling in the TDDFT calculations, so that these transitions do not contribute to the overall spectral profile.

Table 8
Half-wave redox potentials (vs Ag/AgCl) of **1**–**5** at 25 °C.

Complex	$E_1^{1/2,\ ox}$/V[a] (ΔE_p/mV)[b]	$E_2^{1/2,\ ox}$/V[a] (ΔE_p/mV)[b]	$E_1^{1/2,\ red}$/V[a] (ΔE_p/mV)[b]
1	0.71 (57)	0.93 (79)	
2[c]	1.01 (91)		−1.26 (204)
3	0.97 (65)	1.22 (81)	
4	0.68 (52)	0.93 (87)	
5	0.67 (68)	0.92 (79)	

[a] Recorded in dichloromethane solution containing 0.001M iridium complexes, $E_{1/2} = 1/2(E_{pa}+E_{pc})$, where E_{pa} and E_{pc} are anodic and cathodic peak potentials, respectively.
[b] $\Delta E_p = E_{pa}-E_{pc}$.
[c] The second oxidation is not observed for this complex. However, only for this complex a reduction wave is observed.

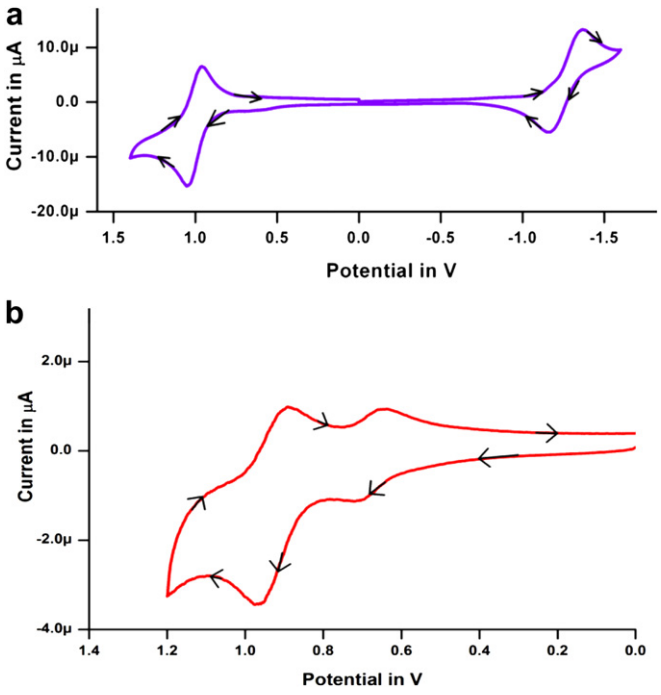

Fig. 6. a): Cyclic voltammogram of **2**, b): Cyclic voltammogram of **5**.

All computations were performed using Gaussian 03 package [29]. Software Gaussum was used to calculate the fractional contributions of various groups to each molecular orbital and also for electronic spectrum simulation with fwhm = 0.4eV [30]. Similar calculations were performed for **3.**

4.5. Synthesis

The chloro-bridged precursor complex $[(ppy)_2Ir(\mu\text{-}Cl)]_2$ was synthesized according to Nonoyama route [31], by refluxing $IrCl_3.nH_2O$ with 2.5 equiv of 2-phenyl pyridine (cyclometalating ligand) in a 3:1 mixture of 2-ethoxyethanol and water. All the ligands (LH, LH–NO_2, LH–CH_3, LH–Cl and LH–F) were synthesized following reported methods [32] by the condensation of picolinic acid with substituted anilines. The complexes **1**–**5** were prepared using an identical synthetic procedure. The synthesis of **1** is outlined below in detail.

4.5.1. $[(ppy)_2Ir(L)]$ (1)

In a 100 mL round bottomed flask $[(ppy)_2\ Ir(\mu\text{-}Cl)]_2$ (0.10 g, 0.093 mmol) was taken along with 30 mL of dichloromethane. To this was added solid sodium methoxide (0.025 g, 0.46 mmol) and the reaction mixture was allowed to stir at room temperature for about 1 h. At this point the solution was orange in color. To this solution was added at once LH (0.046 g, 0.23 mmol) and the reaction mixture was continued to stir at room temperature for 12 h. The progress of the reaction was monitored by TLC by following the disappearance of $[(ppy)_2Ir(\mu\text{-}Cl)]_2$.(eluant: ethylacetate : petroleum ether (60–80 °C) 30:70 (V:V)). The reaction mixture was then filtered and the solvent removed in vacuo to afford a yellow oil. To this was added diethyl ether (10 mL) and triturated affording a yellow solid. This was filtered and washed with cold methanol. The residue was recrystallized from dichloromethane by layering the solution with a few drops of methanol to give compound **1** as yellow crystals. (0.081 g, Yield: 62%).

Characterization data: Anal.Calcd. for $C_{34}H_{25}IrN_4O$: C, 58.52; H, 3.61; N, 8.03. Found: C, 58.44; H, 3.66; N, 8.08. IR(KBr, λ_{max}/cm^{-1}):

3031m, 2923m, 2853w, 1740w, 1607s, 1579vs, 1554s, 1476s, 1437w, 1415m, 1358m, 1304w, 1288w, 1266m, 1225w, 1156m, 1028m, 944w, 811w, 793w, 760vs, 740s, 730s, 691m, 629w, 590w, 505w. ^{1}H NMR (500 MHz, $CDCl_3$) δ: 6.05 (d, J = 7.3 Hz, 1H), 6.42–6.47 (m, 2H), 6.56 (t, J = 7.3 Hz, 1H), 6.63–6.67 (m, 2H), 6.72–6.75 (m, 2H), 6.79–6.85 (m, 1H), 6.91–6.94 (m, 2H), 7.10 (t, J = 6. 7 Hz, 1H), 7.18–7.25 (m, 3H), 7.62–7.74 (m, 6H), 7.82–7.87 (m, 2H), 8.37 (d, J = 7.7 Hz, 1H), 9.05 (d, J = 6Hz, 1H). ESI-MS (100% Acetonoitrile): m/z = 699.16, $[M + H]^+$.

4.5.2. [(ppy)$_2$Ir(L–NO$_2$)] (2)

Quantities: [(ppy)$_2$ Ir(μ-Cl)]$_2$ (0.10 g, 0.093 mmol), sodium methoxide (0.025 g, 0.46 mmol), LH–NO_2 (0.056 g, 0.23 mmol). Yield of **2**:0.094 g, Yield: 68%.

Characterization data: Anal.Calcd. for $C_{34}H_{24}IrN_5O_3$: C, 54.98; H, 3.26; N, 9.43. Found; C, 54.55; H, 3.31; N, 9.27. IR(KBr, λ_{max}/cm^{-1}): 3060w, 2924s, 2854m, 1689w, 1598s, 1495vs, 1415w, 1328vs, 1290m, 1245vs, 1174w, 1121m, 1110m, 1039m, 932w, 841w, 754vs, 712m, 691m, 629w, 438w, 413w. ^{1}H NMR (500 MHz, $CDCl_3$) δ: 6.08 (d, J = 7.2 Hz, 1H), 6.38 (d, J = 7.6 Hz, 1H), 6.63–6.70 (m, 5H), 6.81 (t, J = 7.2 Hz, 1H), 6.95 (t, J = 6.9 Hz, 2H), 7.11–7.13 (m, 2H), 7.20 (d, J = 7.6 Hz, 1H), 7.58–7.67 (m, 5H), 7.75 (m, 2H), 7.88 (d, J = 8.0 Hz, 2H), 8.37 (d, J = 7.6 Hz, 1H), 8.90 (d, J = 5.35 Hz, 1H). ESI-MS (100% Methanol): m/z = 744.15, $[M + H]^+$.

4.5.3. [(ppy)$_2$Ir(L–CH$_3$)] (3)

Quantities used: [(ppy)$_2$ Ir(μ-Cl)]$_2$ (0.10 g, 0.093 mmol), sodium methoxide (0.025 g, 0.46 mmol), L–CH_3 (0.049 g, 0.23 mmol). Yield of **3**: 0.078g, 59%.

Characterization data: Anal.Calcd for $C_{35}H_{27}IrN_4O$: C, 59.06; H, 3.82; N, 7.87. Found; C, 58.72; H, 3.86; N, 7.57. IR(KBr, λ_{max}/cm^{-1}): 3037m, 2993w, 2918w, 1608s, 1580vs, 1558s, 1504m, 1474s, 1436w, 1413s, 1359s, 1314w, 1302w, 1291w, 1266m, 1255w, 1224w, 1158m, 1123w, 1110w, 1090w, 1061w, 1049w, 1029m, 1015w, 945w, 923w, 907w, 806w, 794w, 761vs, 748m, 735s, 712w, 695w, 683w, 668w, 629w, 543w, 524w, 496w, 472w, 422w. ^{1}H NMR (500 MHz, $CDCl_3$) δ: 2.06 (s, 3H), 6.04 (d, J = 7.6 Hz, 1H), 6.35 (d, J = 8.4 Hz, 3H), 6.41(d, J = 7.25 Hz, 1H), 6.53–6.57 (m, 2H), 6.64–6.65(m, 1H), 6.81–6.83 (m, 3H), 6.91–6.94 (m, 2H), 7.08–7.09(m, 1H), 7.17–7.19 (m, 1H), 7.61–7.72 (m, 5H), 7.82–7.87(m, 2H), 8.36 (d, J = 7.6 Hz, 1H), 9.03 (d, J = 5.35 Hz, 1H). ESI-MS (100% Acetonitrile): m/z = 713.15, $[M + H]^+$.

4.5.4. [(ppy)$_2$Ir(L–Cl)] (4)

Quantities used:[(ppy)$_2$Ir(μ-Cl)]$_2$ (0.10 g, 0.093 mmol), sodium methoxide (0.025 g, 0.46 mmol), L–Cl (0.054 g, 0.23 mmol). Yield of **4**: 0.091 g, 67%.

Characterization data: Anal.Calcd. for $C_{34}H_{24}ClIrN_4O$: C, 55.77; H, 3.30; N, 7.65. Found; C, 55.53; H, 3.30; N, 7.42. IR(KBr, λ_{max}/cm^{-1}): 3038w, 2998w, 2923w, 1872w, 1609s, 1581vs, 1560s, 1478s, 1437s, 1415s, 1358s, 1292w, 1266w, 1257w, 1225w, 1160w, 1050w, 1029m, 1010w, 947w, 923w, 907w, 816w, 794w, 761vs, 737s, 704w, 692w, 669w, 629w, 517w, 475w, 424w. ^{1}H NMR (500 MHz, $CDCl_3$) δ: 6.05 (d, J = 7.65 Hz, 1H), 6.41–6.44 (m, 3H), 6.60 (t, J = 7.25 Hz, 1H), 6.67–6.70 (m, 2H), 6.80–6.83 (m, 2H), 6.92–6.95 (m, 2H), 7.08–7.11 (m, 1H), 7.19–7.22 (m, 1H), 7.25–7.26 (m, 2H), 7.63–7.66 (m, 3H), 7.70–7.73 (m, 2H), 7.83–7.86 (m, 2H), 8.35 (d, J = 7.6 Hz, 1H), 8.95 (d, J = 5.7 Hz, 1H). ESI-MS (100% methanol): m/z = 733.15, $[M + H]^+$.

4.5.5. [(ppy)$_2$Ir(L–F)] (5)

Quantities used: [(ppy)$_2$Ir(μ-Cl)]$_2$ (0.1 g, 0.093 mmol), sodium methoxide (0.025 mg, 0.46 mmol), L–F (0.050 g, 0.23 mmol). Yield of **5**: 0.084 g, 63%.

Characterization data: Anal.Calcd. for $C_{34}H_{24}FIrN_4O$: C, 57.05; H, 3.38; N, 7.83. Found; C, 56.94; H, 3.38; N, 7.4. IR(KBr, λ_{max}/cm^{-1}): 3031w, 2924m, 2853w, 1609s, 1579vs, 1500s, 1476s, 1438w, 1416m, 1372m, 1305w, 1290w, 1267w, 1216m, 1150w, 1091w, 1062w, 1030w, 1010w, 943w, 821m, 784w, 759vs, 732s, 693w, 629w, 541w, 527w, 476w. ^{1}H NMR (500 MHz, $CDCl_3$) δ: 6.05 (d, J = 7.6 Hz, 1H), 6.40–6.44(m, 5H), 6.58 (t, J = 7.6 Hz, 1H), 6.67 (t, J = 7.6 Hz, 1H), 6.79–6.83 (m, 2H), 7.09 (t, J = 7.2 Hz, 1H), 7.18–7.25 (m, 3H), 7.62–7.73 (m, 6H), 7.86 (d, J = 6.5 Hz, 2H), 8.35 (d, J = 8.0 Hz, 1H), 8.97 (d, J = 5.3 Hz, 1H). ESI-MS (100% methanol): m/z = 717.16, $[M + H]^+$.

Acknowledgement

We thank the Department of Science and Technology (DST), India for financial support. B.M. and P.B. are thankful to CSIR, New Delhi, India for Fellowship. We also thank Dr. Pratik Sen (IIT Kanpur) for valuable suggestions and R. Suriya Narayanan for TGA studies.

Appendix A. Supplementary material

CCDC numbers 784721 – 784724 (**1**, **3**, **4**, and **5**) contains the supplementary crystallographic data for this paper. These data can be obtained free of charge from The Cambridge Crystallographic Data Centre www.ccdc.cam.ac.uk/data_request/cif.

Appendix. Supplementary data

Supplementary data associated with this article can be found, in the online version, at doi:10.1016/j.jorganchem.2011.04.011.

References

[1] (a) L. Flamigni, A. Barbieri, C. Sabatini, B. Ventura, F. Barigelletti, Top. Curr. Chem. 281 (2007) 143–204;
(b) I.M. Dixon, J.P. Collin, J.P. Sauvage, L. Flamigni, S. Encinas, F. Barigelletti, Chem. Soc. Rev. 29 (2000) 385–391.
[2] (a) C. Adachi, M.A. Baldo, S.R. Forrest, M.E. Thompson, Appl. Phys. Lett. 77 (2000) 904–906;
(b) M.A. Baldo, S. Lamansky, P.E. Burrows, M.E. Thompson, S.R. Forrest, Appl. Phys. Lett. 75 (1999) 4–6;
(c) P.T. Chou, Y. Chi, Chem. Eur. J. 13 (2007) 380–395.
[3] (a) R.C. Evans, P. Douglas, C.J. Winscom, Coord. Chem. Rev. 250 (2006) 2093–2126;
(b) M. Nazeeruddin, R.T. Wegh, Z. Zhou, C. Klein, Q. Wang, F. De. Angelis, S. Fantacci, M. Grätzel, Inorg. Chem. 45 (2006) 9245–9250;
(c) D. Di. Censo, S. Fantacci, F. De. Angelis, C. Klein, N. Evans, K. Kalyanasundaram, H.J. Bolink, M. Grätzel, M.K. Nazeeruddin, Inorg. Chem. 47 (2008) 980–989;
(d) H.J. Bolink, L. Cappelli, E. Coronado, M. Grätzel, E. Orti, R.D. Costa, P.M. Viruela, M.K. Nazeeruddin, J. Am. Chem. Soc. 128 (2006) 14786–14787.
[4] (a) M.M. Richter, Chem. Rev. 104 (2004) 3003–3036;
(b) A. Kapturkiewicz, G. Angulo, Dalton Trans. (2003) 3907–3913.
[5] J.I. Goldsmith, W.R. Hudson, M.S. Lowry, T.H. Anderson, S. Bernhard, J. Am. Chem. Soc. 127 (2005) 7502–7510.
[6] (a) Y. Chi, P.T. Chou, Chem. Soc. Rev. 36 (2007) 1421–1431;
(b) E.I. Mayo, K. Kilsa, T. Tirrell, P.I. Djurovich, A. Tamayo, M.E. Thompson, N.S. Lewis, H.B. Gray, Photochem. Photobiol. Sci. 5 (2006) 871–873.
[7] (a) M.X. Yu, Q. Zhao, L.X. Shi, F.Y. Li, Z.G. Zhou, H. Yang, T. Yia, C.H. Huang, Chem. Commun. (2008) 2115–2117;
(b) K.K. Lo, K.K.W. Lo, J.S.Y. Lau, Inorg. Chem. 46 (2007) 700–709;
(c) K.K.W. Lo, K.Y. Zhang, C.K. Chung, K.Y. Kwok, Chem. Eur. J. 13 (2007) 7110;
(d) K.K.W. Lo, C.K. Chung, N. Zhu, Chem.Eur. J. 12 (2006) 1500–1512.
[8] (a) T. Liu, B.H. Xia, Q.C. Zheng, X. Zhou, Q.J. Pan, H.X. Zhang, J. Comput. Chem. 31 (2010) 628–638;
(b) P.J. Hay, J. Phys. Chem. A 106 (2002) 1634–1641;
(c) M.S. Lowry, S. Bernard, Chem. Eur. J. 12 (2006) 7970–7977;
(d) T.H. Kwon, H.S. Cho, M.K. Kim, J.W. Kim, J.J. Kim, K.H. Lee, S.J. Park, I.S. Shin, H. Kim, D.M. Shin, Y.K. Chung, J.I. Hong, Organometallics 24 (2005) 1578–1585.
[9] (a) A. Tsuboyama, H. Iwawaki, M. Furugori, T. Mukaide, J. Kamatani, S. Igawa, T. Moriyama, S. Miura, T. Takiguchi, S. Okada, M. Hoshino, K. Ueno, J. Am. Chem. Soc. 125 (2003) 12971–12979;
(b) T. Sajoto, P.I. Djurovich, A. Tamayo, M. Yousufuddin, R. Bau, M.E. Thompson, R.J. Holmes, S.R. Forrest, Inorg. Chem. 44 (2005) 7992–8003;

(c) A.B. Tamayo, B.D. Alleyne, P.I. Djurovich, S. Lamansky, I. Tsyba, N.N. Ho, R. Bau, M.E. Thompson, J. Am. Chem. Soc. 125 (2003) 7377–7387.
[10] (a) B. Liang, C.Y. Jiang, Z. Chen, X.J. Zhang, H.H. Shi, Y. Cao, J. Mater. Chem. 16 (2006) 1281–1286;
(b) Z.W. Liu, M. Guan, Z.Q. Bian, D.B. Nie, Z.L. Gong, Z.B. Li, C.H. Huang, Adv. Funct. Mater. 16 (2006) 1441–1448;
(c) Y.H. Song, S.J. Yeh, C.T. Chen, Y. Chi, C.S. Liu, J.K. Yu, Y.H. Hu, P.T. Chou, S.M. Peng, G.H. Lee, Adv. Funct. Mater. 14 (2004) 1221–1226;
(d) C.F. Chang, Y.M. Cheng, Y. Chi, Y.C. Chiu, C.C. Lin, G.H. Lee, P.T. Chou, C.C. Chen, C.H. Chang, C.C. Wu, Angew. Chem. Int. Ed. 47 (2008) 4542–4545;
(e) E. Orselli, G.S. Kottas, A.E. Konradsson, P. Coppo, R. Fröhlich, L. De Cola, A. van Dijken, M.H. Börner, Inorg. Chem. 46 (2007) 11082–11093;
(f) C.H. Yang, Y.M. Cheng, Y. Chi, C.J. Hsu, F.C. Fang, K.T. Wong, P.T. Chou, C.H. Chang, M.H. Tsai, C.C. Wu, Angew. Chem. Int. Ed. 46 (2007) 2418–2421;
(g) R. Ragni, E.A. Plummer, K. Brunner, J.W. Hofstraat, F. Babudri, G.M. Farinola, F. Naso, L. De Cola, J. Mater. Chem. 16 (2006) 1161–1170;
(h) C.H. Yang, S.W. Li, Y. Chi, Y.M. Cheng, Y.S. Yeh, P.T. Chou, G.H. Lee, C.H. Wang, C.F. Shu, Inorg. Chem. 44 (2005) 7770–7780;
(i) C. Dragonetti, L. Falciola, P. Mussini, S. Righetto, D. Roberto, R. Ugo, A. Valore, F. De Angelis, S. Fantacci, A. Sgamellotti, M. Ramon, M. Muccini, Inorg. Chem. 46 (2007) 8533–8547;
(j) Q. Zhao, S. Liu, M. Shi, C. Wang, M. Yu, L. Li, F. Li, T. Yi, C. Huang, Inorg. Chem. 45 (2006) 6152–6160;
(k) A.B. Tamayo, S. Garon, T. Sajoto, P.I. Djurovich, I.M. Tsyba, R. Bau, M.E. Thompson, Inorg. Chem. 44 (2005) 8723–8732;
(l) Md.K. Nazeeruddin, R. Humphry-Baker, D. Berner, S. Rivier, L. Zuppiroli, M. Grätzel, J. Am. Chem. Soc. 125 (2003) 8790–8797.
[11] (a) G. Volpi, C. Garino, L. Salassa, J. Fiedler, K.I. Hardcastle, R. Gobetto, C. Nervi, Chem. Eur. J. 15 (2009) 6415–6427;
(b) Y. You, S.Y. Park, J. Am. Chem. Soc. 127 (2005) 12438–12439;
(c) Wei Yang, Hao Fu, Qijun Song, Min Zhang, Yuqiang Ding, Organometallics 30 (2011) 77–83 (During the preparation of this manuscript this article appeared).
[12] (a) D.W. Margerum, Pure Appl. Chem. 55 (1983) 23–24;
(b) T.J. Collins, Acc. Chem. Res. 35 (2002) 782–790;
(c) M.J. Bartos, S.W. Gordon-Wylie, B.G. Fox, L.J. Wright, S.T. Weintraub, K.E. Kauffmann, E. Münck, K.L. Kosta, E.S. Uffelman, C.E.F. Rickard, K.R. Noon, T.J. Collins, Coord. Chem. Rev. 174 (1998) 361–390;
(d) T.J. Collins, Acc. Chem. Res. 27 (1994) 279–285;
(e) M.H. Chou, D.J. Szalda, C. Creutz, N. Sutin, Inorg. Chem. 33 (1994) 1674–1684;
(f) P.C. Ford, D.P. Rudd, R. Gaunder, H. Taube, J. Am. Chem. Soc. 90 (1968) 1187–1194;
(g) A.K. Singh, V. Balamurugan, R. Mukherjee, Inorg. Chem. 42 (2003) 6497–6502;
(h) H. Sigel, Inorg. Chem. 14 (1975) 1535–1540;
(i) H. Sigel, C.F. Naumann, B. Prijs, D.B. McCormick, M.C. Falk, Inorg. Chem. 16 (1977) 790–796;
(j) M.F. El-Shazly, El. Dissowky, T. Salem, M. Osman, Inorg. Chim. Acta 40 (1980) 1–6;
(k) A. White, X. Ding, J.C. vanderSpek, J.R. Murphy, D. Ringe, Nature 394 (1998) 502–506;
(l) E. Pohl, R.K. Holmes, W.G.J.J. Hol, Mol. Biol. 292 (1999) 653–667;
(m) S.H.V. Rijt, A. Hebden, T. Amaresekera, R.J. Deeth, G.J. Clarkson, S. Parsons, P.C. McGowan, P.J. Sadler, J. Med. Chem. 52 (2009) 7753–7764.
[13] (a) P. Srinivas, P.R. Likhar, H. Maheswaran, B. Sridhar, K. Ravikumar, M.L. Kantam, Chem. Eur. J. 15 (2009) 1578–1581;
(b) M.L. Kantam, P. Srinivas, J. Yadav, P.R. Likhar, S. Bhargava, J. Org. Chem. 74 (2009) 4882–4885.
[14] (a) S. Lamansky, P. Djurovich, D. Murphy, F. Abdel-Razzaq, R. Kwong, I. Tsyba, M. Bortz, B. Mui, R. Bau, M.E. Thompson, Inorg. Chem. 40 (2001) 1704–1711;
(b) J. Breu, P. Stossel, S. Schrader, A. Starukhin, W.J. Finkenzeller, H. Yersin, Chem. Mater 17 (2005) 1745–1757;
(c) D.G.H. Hetterscheid, J. Kaiser, E. Reijerse, T.P.J. Peters, S. Thewissen, A.N.J. Blok, J.M.M. Smits, R. De. Gelder, B. De. Bruin, J. Am. Chem. Soc. 127 (2005) 1895–1905.
[15] S. Lamansky, P. Djurovich, D. Murphy, F. Abdel-Razzaq, H.E. Lee, C. Adachi, P.E. Burrows, S.R. Forrest, M.E. Thompson, J. Am. Chem. Soc. 123 (2001) 4304–4312.
[16] (a) M. Lepeltier, T.K.M. Lee, K.K.W. Lo, L. Toupet, H. Le Bozec, V. Guerchais, Eur. J. Inorg. Chem. (2005) 110–117;
(b) W.S. Sie, J.Y. Jian, T.C. Su, G.H. Lee, H.M. Lee, K.B. Shiu, J. Org. Chem. 693 (2008) 1510–1517.
[17] (a) M.G. Colombo, A. Hauser, H.U. Guedel, Inorg. Chem. 32 (1993) 3088–3092;
(b) L. Flamigni, B. Ventura, F. Barigelletti, E. Baranoff, J.P. Collin, J.P. Sauvage, Eur. J. Inorg. Chem. (2005) 1312–1318;
(c) J.P. Collman, C.E. Barnes, P.N. Swepston, J.A. Ibers, J. Am. Chem. Soc. 106 (1984) 3500–3510;
(d) J. Li, P.I. Djurovich, B.D. Alleyne, M. Yousufuddin, N.N. Ho, J.C. Thomas, J.C. Peters, R. Bau, M.E. Thompson, Inorg. Chem. 44 (2005) 1713–1727.
[18] (a) X. Ren, D.J. Giesen, M. Rajeswaran, M. Madaras, Organometallics 28 (2009) 6079–6089;
(b) S. Nag, R. Butcher, S. Bhattacharya, Eur. J. Inorg. Chem. (2007) 1251–1260.
[19] (a) W.H. Smith, A.J. Bard, J. Am. Chem. Soc. 97 (1975) 5203–5210;
(b) A.S. Mendkovich, L.V. Michalchenko, V.P. Gultyai, J. Electroanal. Chem. 224 (1987) 273.
[20] A.I. Vogel, Vogel's Textbook f Practical Organic Chemistry, fifth ed. Longman, London, 1989.
[21] (a) I.B. Berlman, Handbook of Fluorescence Spectra of Aromatic Molecules. Academic Press, New York, 1965;
(b) W.H. Melhuish, J. Phys. Chem. 65 (1961) 229.
[22] Smart & SAINT Software Reference Manuals, Version 6.45. Bruker Analytical X-ray Systems, Inc., Madison, WI, 2003.
[23] G.M. Sheldrick, SADABS, a Software for Empirical Absorption Correction, Version. 2.05. University of Göttingen, Göttingen, Germany, 2002.
[24] (a) G.M. Sheldrick, SHELXTL Reference Manual, Version. 6.1. Bruker Analytical X-ray Systems, Inc., Madison, WI, 2000;
(b) G.M. Sheldrick, SHELXTL Ver. 6.12. Bruker Analytical X-ray Systems, Inc., Madison, WI, 2001.
[25] (a) C. Lee, W. Yang, R.G. Parr, Phys. Rev. B 37 (1988) 785–789;
(b) A.D. Becke, J. Chem. Phys. 98 (1993) 5648–5653.
[26] J.P. Perdew, K. Burke, M. Ernerhof, Phys. Rev. Lett. 78 (1997) 1396.
[27] (a) P.J. Hay, W.R. Wadt, J. Chem. Phys. 82 (1985) 299–310;
(b) P.J. Hay, W.R. Wadt, J. Chem. Phys. 82 (1985) 270–283.
[28] (a) V. Barone, M. Cossi, J. Chem. Phys. 107 (1997) 3210–3221;
(b) M. Cossi, G. Scalmani, N. Regar, V. Barone, J. Chem. Phys. 117 (2002) 43–54.
[29] M.J. Frisch, G.W. Trucks, H.B. Schlegel, G.E. Scuseria, M.A. Robb, J.R. Cheeseman, J.A. Montgomery Jr., T. Vreven, K.N. Kudin, J.C. Burant, J.M. Millam, S.S. Iyengar, J. Tomasi, V. Barone, B. Mennucci, M. Cossi, G. Scalmani, N. Rega, G.A. Petersson, H. Nakatsuji, M. Hada, M. Ehara, K. Toyota, R. Fukuda, J. Hasegawa, M. Ishida, T. Nakajima, Y. Honda, O. Kitao, H. Nakai, M. Klene, X. Li, J.E. Knox, H.P. Hratchian, J.B. Cross, C. Adamo, J. Jaramillo, R. Gomperts, R.E. Stratmann, O. Yazyev, A.J. Austin, R. Cammi, C. Pomelli, J. Ochterski, P.Y. Ayala, K. Morokuma, G.A. Voth, P. Salvador, J.J. Dannenberg, V.G. Zakrzewski, S. Dapprich, A.D. Daniels, M.C. Strain, O. Farkas, D.K. Malick, A.D. Rabuck, K. Raghavachari, J.B. Forestman, J.V. Ortiz, Q. Cui, A.G. Baboul, S. Clifford, J. Cioslowski, B.B. Stefanov, G. Liu, A. Liashenko, P. Piskorz, I. Komaromi, R.L. Martin, D.J. Fox, T. Keith, M.A. Al-Laham, C.Y. Peng, A. Nanayakkara, M. Challacombe, P.M.W. Gill, B. Johnson, W. Chen, M.W. Wong, C. Gonzales, J.A. Pople, Gaussian 03, Revision D.01. Gaussian Inc., Wallingford CT, 2004.
[30] N.M. O'Boyle, A.L. Tenderholt, K.M. Langner, J. Comp. Chem. 29 (2008) 839–845.
[31] M. Nonoyama, Bull. Chem. Soc. Jpn. 47 (1974) 767–768.
[32] S. Dutta, S. Pal, P.K. Bhattacharya, Polyhedron 18 (1999) 2157–2162.